

Development of Determination Methodology of Electrical Conductivity of Titanium-Based Composites

Donatas GRICIUS*, Rasa KANDROTAITĖ JANUTIENĖ**, Darius MAŽEIKA***, Rolandas ŠERTVYTIS****, Olha SYZONENKO*****, Andrii TORPAKOV*****

*Kaunas University of Technology, Studentų st. 56, 51424 Kaunas, Lithuania, E-mail: donatas.gricius@ktu.edu

**Kaunas University of Technology, Studentų st. 56, 51424 Kaunas, Lithuania, E-mail: raskand@ktu.lt

***Kaunas University of Technology, Studentų st. 56, 51424 Kaunas, Lithuania, E-mail: darius.mazeika@ktu.lt

****Kaunas University of Technology, Studentų st. 56, 51424 Kaunas, Lithuania, E-mail: rolandas.sertvytis@ktu.lt

*****Institute of Pulse Processes and Technologies of NAS of Ukraine, Bohoyavlenskyi ave., 43-A, 54018, Mykolaiv, Ukraine, E-mail: sizonenko43@rambler.ru

*****Institute of Pulse Processes and Technologies of NAS of Ukraine, Bohoyavlenskyi ave., 43-A, 54018, Mykolaiv, Ukraine, E-mail: torpakov@gmail.com

<https://doi.org/10.5755/j02.mech.32230>

1. Introduction

Titanium-based (Ti-based) metal matrix composites are novel materials that have superior mechanical properties. These composites have potential to be used in the aviation industry for their good specific strength, lightweight, heat and wear resistance [1]. They are already used in aircraft engines and gas turbines [1, 2]. Determination of material properties of these novel composites require further studies and experimental tests. One of the important properties is electrical conductivity. To measure electrical conductivity, a measurement setup suitable for composite samples is needed.

Like metals, Ti-based composites are good electrical conductors. They have an electrical conductivity in the range of 10^6 S/m [3, 4]. The electrical conductivity of a composite depends on many factors, such as chemical composition, particle size, porosity, homogeneity, isotropy, and manufacturing method. The Ti-based composites are manufactured using high voltage electrical discharge (HVED) and spark plasma sintering (SPS) methods from powders. After HVED process composite contains carbides and MAX phases [2, 3]. In addition, the particle size is reduced and all components are distributed evenly [2]. Porosity inside the microstructure occurs due to air bubbles that appear during manufacturing and interaction between matrix and reinforcement particles [4]. The optimal ratio between the constituent components at which both electrical and mechanical properties are optimal is important to find. Most powder based metal matrix composites are isotropic in nature [5]. Four point probe method is commonly used to measure electrical conductivity of such composite samples [3, 4]. When utilizing this method, the sample geometry must be considered, and appropriate corrections must be made. Ideally, test sample should have uniform geometry and thickness. Sample test surface should be polished and cleaned to minimize surface roughness, pores and contaminants [4]. The probes must contact the sample with small probes arranged in a straight line. Two outer probes have current running through them, and two inner probes measure potential difference. This method eliminates parasitic resistance coming out of the probe contact. The force of probes into sample should be constant and equal with all probes [6, 7]. The electrical conductivity dependence on temperature is an important

characteristic. Sample heaters or coolers are commonly used in measurement setups. It is known that electrical conductivity increases at lower temperature. Furthermore, measurements under controlled atmosphere for instance vacuum eliminates errors coming from humidity. The current source applied should be pulsed DC or AC to prevent Joule heating of the sample, which could influence the result. Voltage measurements must be conducted with sensitive nanovoltmeter. Outside interference that could affect measurement must be considered.

This work will advance knowledge about electrical conductivity properties of Ti-based metal matrix composites. Improved ways for measuring electrical conductivity of metal matrix composites are proposed. In addition, experimental data of electrical conductivity for bulk-pellet-shape samples of finite geometry is acquired. Research for such shape composite samples is limited. The influence of outside factors such as temperature and atmosphere are researched.

The aim of the research is to develop and test an experimental setup for measuring electrical conductivity of titanium metal matrix composites. Designed experimental setup was comparatively tested using standard copper sample.

2. Methodology

The probes that are used for experimental setup are made of spring steel and gold plated [8]. The yield strength of the material of the probe is 525 MPa.

Fig. 1 presents the schema of a probe and its geometrical parameters (Fig. 1).

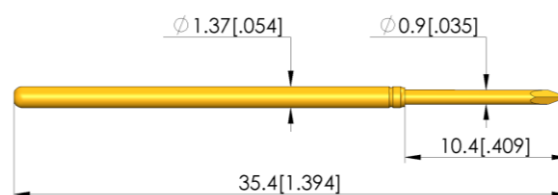


Fig. 1 A probe used for designing of experimental setup [8]

The tested samples in this research have a cylinder pellet shape, variance from approximately 10.05 to

10.35 mm diameter and 4.75 to 6.45 mm thickness. Samples do not have a perfect shape, variations in thickness and diameter occurs when measuring the height and the thickness of every sample (Table 1).

Table 1

Geometrical parameters of samples

Sample	Diameter, mm	Thickness, mm
N6	10.35	4.75
N7	10.1	6.45
N8	10.05	5.6
N10	10.1	6.4
G6	10.1	5.5
G7	10.2	4.9

The data on the research of electrical conductivity of similar composite materials is summarized and presented.

Table 2 shows a comparison of properties of the composite materials from other similar scientific researches.

Table 2

Comparison of Ti-Al-C composites properties

Material	Electrical conductivity, S/m	Measurement method	Manufacturing method	Reference
TiC - 10 wt. % Ti ₃ Al	1.2·10 ⁵	Kelvin 4 wire with AC resistance bridge	Pressure less sintering at 1500 °C	[9]
Ti ₂ AlC and Ti ₃ AlC ₂	1.85·10 ⁶	Linear Van der Pauw	Magnetron sputtering, annealing at 850 °C	[10]
Ti ₂ AlC - 5 wt. % TiC	1.63·10 ⁶	Four-probe	Sintering at 1350 °C	[3]
Ti ₃ AlC ₂ - 5 vol. % Al ₂ O ₃	3.05·10 ⁶	Four-probe	Sintered at 1400°C	[4]
Ti ₃ AlC ₂	1.22·10 ⁵	DC four-probe	Sintered in vacuum at 1400°C	[11]

The lowest resistivity obtained was $0.327 \cdot 10^{-6} \Omega\text{m}$ and highest $8.3 \cdot 10^{-6} \Omega\text{m}$. Most of the measurements performed with four-probe method under the room temperature and air atmosphere.

In Fig. 2 presents a Solidworks model of the measurement set used in this study. Fig. 3 presents a real view of a designed experimental setup, connected to the Arduino board.

The sample is placed inside the sample holder and fixed by tightening screw. In addition, thermal paste is applied on the side, which will encounter the Peltier module. The thermal paste has two functions, increasing surface area and allowing the sample to lay flat despite thickness irregularities. A small gap is left between the sample holder and Peltier module fixation part. Both parts are made of isolative material and are fixed flat by four screws. The Peltier module is fixed inside the bottom part and is attached directly to the sample on one side and to an aluminium block to the other. The aluminium block serves as a heat dissipater to increase the cooling rate. The aluminium block slides on four metal rods that serve as guides for movement in one direction. Metal rods are greased with oil to reduce friction.

The metal block moves up and down because of a hydraulic cylinder. Movement occurs from bottom to up and prevents bending of needles due to surface roughness of the sample. The cylinder has a 50 mm travel and travel speed of 3 mm/s. Arduino board controls the cylinder travel and the feedback goes to controller once test needles touch the sample; cylinder stops after a second. This ensures equal amount of pressure is exerted on the samples every time despite different thicknesses. The load of 2 N is applied on every needle generating by spring. Such a load of 2 N occurs when the displacement is 4.3 mm. The stiffness of springs is 0.65 N/mm [8]. Specification presented by producer states that the main material of probes is steel coated with gold [8]. The needles have a sharp tip that can penetrate oxide layer. Proper contact to sample and equal pressure is ensured. Adjacent needles have 2 mm distance between each other. Needles are pressed into the needle holder part which is made of an isolative material. The needle holder is pressed into a metal part, which is also connected with guiding metal rods. The top metal part is fixed to housing with bolts and nuts. The housing and whole assembly has 170 x 120 x 280 mm dimensions.

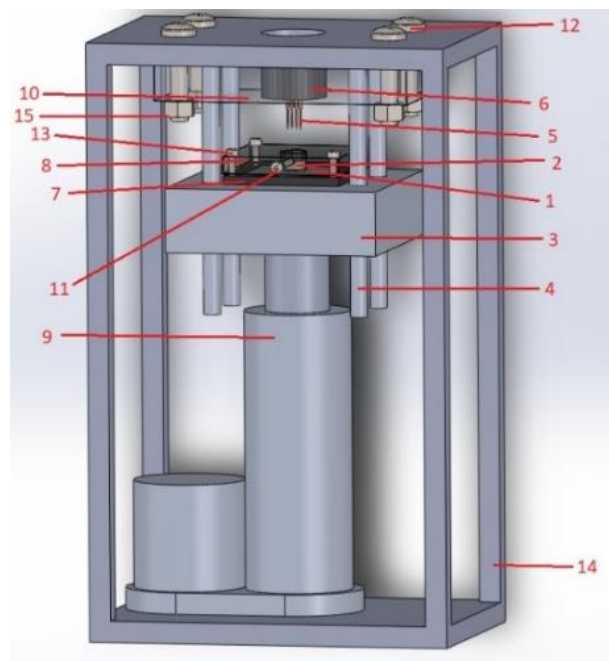


Fig. 2 Solidworks model of electrical conductivity measurement setup: 1 – Peltier module; 2 – sample; 3 – cooling block; 4 – cylinder; 5 – needle probes; 6 – probe holder; 7 – Peltier module holder; 8 – sample holder; 9 – linear motion drive; 10 – top fixation part; 11 – M3 fixation screw; 12 – M8 bolt; 13 – M3 screw; 14 – frame; 15 – M8 nut

A Keithley 2614b source meter was used as a current source and voltage measurement tool. Voltage measurements were done with pulses. Number of measurements can be selected before test. A mean, standard deviation, minimum and maximum values were given by the meter. Measurements were performed by using 4 wires and ohm-meter mode. Four wire method eliminates resistance coming from probes. A 100 mA current was used for Ti composite samples and 1 A was used for copper sample. The resistance is automatically calculated by the source meter. Accuracy of measurements is 0.03 % + 1.5 mA for current source at 1 A

range, and 0.015 % + 150 μ V for voltage measuring at 100 mV range [8].

A simulation was performed to validate model and better understand current flow. A model was created with Comsol software. Mesh size: from 1.6×10^{-4} m to 0.00128 m. Cylindrical sample has 6 mm height and 10 mm diameter. Two adjacent probes are spaced 2 mm apart. Probe spacing is determined based on the needles and the biggest diameter of the sample. Probe needle tip is not infinitely small; the tip is 0.04 mm diameter. The tip had to be of finite diameter because very small mesh would be needed.

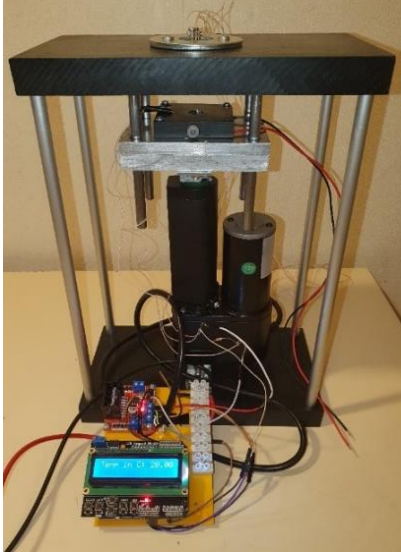


Fig. 3 Fully assembled measurement setup

Electric currents, Joule heating and solid mechanics physics are used in the simulation. Sample and probes are separate entities and form an assembly. Mechanical and electrical contacts are applied to areas where probes touch sample. One probe current is applied point current source of 1 ampere. The other current probe is given ground. Pure titanium material properties are used in simulation because it is the closest material to real samples available. At the positions of the voltage probes, electric potential values are taken. The plot of the simulation can be seen in Fig. 4.

Fig. 4 shows the current paths' distribution around the sample and. It is well known that finite geometry samples resistivity measurements need correction factors [6].

The resistivity without correction factor is calculated by using Eq. (1).

$$\rho = 2 \cdot \pi \cdot s \cdot \left(\frac{U}{I} \right), \quad (1)$$

where: ρ is the resistivity of the sample material, $\Omega \cdot m$; s is the spacing between two adjacent probes, m; I is the current applied between current probes, A.

$$\rho = 2 \cdot 3.14 \cdot 0.002 \cdot \left(\frac{3.8 \cdot 10^{-5}}{1} \right) = 4.77 \cdot 10^{-7} \Omega \cdot m.$$

Resistivity with correction factor is calculated by using Eq. (2). Two correction factors applied that are taken from scientific literature [13, 14].

$$\rho_c = 2 \cdot \pi \cdot s \cdot \left(\frac{U}{I} \right) \cdot F_1 \cdot F_2, \quad (2)$$

where: ρ_c is the resistivity of the sample material with correction factors, $\Omega \cdot m$; F_1 is the correction factor for finite thickness; F_2 is the correction factor for finite lateral width.

$$\rho_c = 2 \cdot 3.14 \cdot 0.002 \cdot \left(\frac{3.8 \cdot 10^{-5}}{1} \right) \cdot 0.978 \cdot 0.7419 = 3.46 \cdot 10^{-7} \Omega \cdot m.$$

The true resistivity of titanium presented in COMSOL software is $3.846 \times 10^{-7} \Omega \cdot m$. Resistivity with correction factor is closer to the true value of the material. The percentage error with correction factor is 10% and 24% without correction factor.

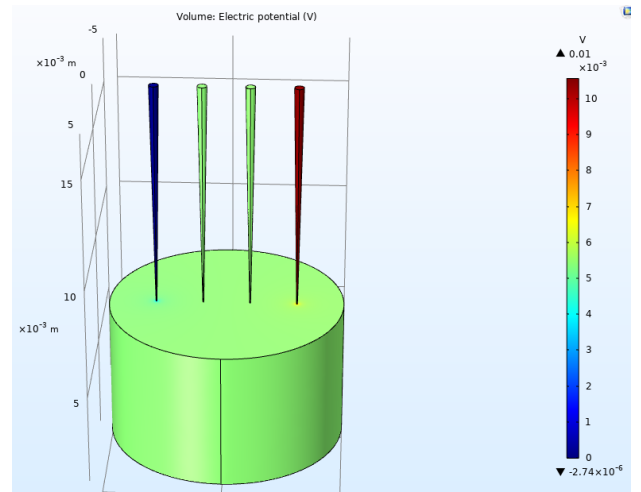


Fig. 4 Electric potential plot of collinear for point probe method from Comsol [12]

4. Results and discussion

A simulation was performed to determine the influence of contact force to the electrical connection of probes and sample. Contact pressure parameter was applied to the contact pair at the connection area. Ideally, probe tip should be infinitely small; in this case, probe tip had radius of 0.02 mm and area of $1.25 \cdot 10^{-9} \text{ m}^2$. The needle probe used in setup will be spring-loaded and will have a force rating. By using Eq. 3, contact pressure can be calculated.

$$P = \frac{F}{A}, \quad (3)$$

where: P is the contact pressure, N/m^2 ; F is the theoretical force of spring-loaded probe, N; A is the area of probe tip, m^2 .

Simulation results are presented in Table 3.

It was found that at least 8 N force is required to have adequate contact. If force is increased further, no change is seen. The resistivity at 8 N force or higher is the same as bonded connection. Below 8 N force, big variation is seen. Resistivity is much smaller than the true value. This indicates that proper connection between probe and sample is not made sufficiently well. This behavior can occur be due

to surface roughness and hardness of the materials. At a certain force, in this case, at 8 N, surface roughness is flattened and an ohmic connection is made.

In Fig. 5, a plot of von Mises stress is shown. During shown simulation 8 N force or $6.39 \cdot 10^9 \text{ N/m}^2$ is applied. The probes were constrained in X and Y directions. The sample was fixed immovably.

Table 3
Contact force simulation results

Contact pressure applied to all four probes, N/m^2	Force on individual probe, N	Resistivity no correction, Ωm	Resistivity with correction, Ωm
$3.99 \cdot 10^9$	5	$2.69 \cdot 10^2$	$1.95 \cdot 10^2$
$6.39 \cdot 10^9$	8	$4.77 \cdot 10^{-7}$	$3.46 \cdot 10^{-7}$
$7.98 \cdot 10^9$	10	$4.77 \cdot 10^{-7}$	$3.46 \cdot 10^{-7}$

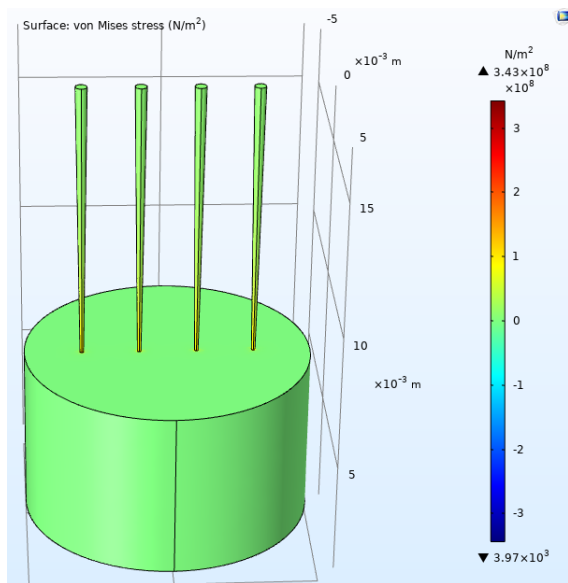


Fig. 5 Von Mises stress plot with 8 N force applied

The highest stresses were calculated at the tip of the probe needle. Maximum stresses are obtained at the very tip that are lower than yield strength (525 MPa) of the material of the probe. The stress in the sample is lower than the yield strength of titanium. In this simulation, both, probes and composite sample would not be plastically deformed. In real scenario, the probe needles would have much sharper tip and lower force would be needed to achieve ohmic contact. However, experimental testing would be needed to find the minimum needed force.

Six titanium-based composite samples were tested in total. One sample was measured six times; every time needle holder was rotated by 45 degrees. Additionally, at each position, 30 measurements were performed by the meter. By using statistics function, mean, standard deviation, minimum and maximum values were calculated automatically by the meter. Furthermore, an average of the six measurements was calculated, the results are presented in Table 4. The Peltier element was used to maintain a constant 20°C of the sample during measurement.

Another test was performed in different temperatures. Measurements were performed without rotating needle holder, only at one position. Peltier element used to heat and cool the sample. Firstly, sample was cooled until tem-

perature reached 10°C . After measuring all the samples, Peltier element was used in heating mode to bring the sample temperature to 50°C . EX355P AIM-TTI programmable power supplied linear drive 12V and Peltier element with needed current and voltage. The resistance measurement results are shown in Fig. 6.

All Ti-based composites either tested by experimental method or found in literature had higher electrical resistivity than pure titanium. This can be explained by the microstructure of the composite. The microstructure has porosity and air gaps that increase the resistivity. Also, different particle material bonding could affect the overall resistivity. Furthermore, the alignment of the particles, whether isotropic or anisotropic affects result. The comparison of highest and lowest values obtained by different methods is presented in Table 5.

Table 4

Measurement results of average electrical resistance

Sample	Mean, Ω	Standard deviation, Ω	Min, $\text{m}\Omega$	Max, $\text{m}\Omega$
N6	$4.11 \cdot 10^{-3}$	$4.28 \cdot 10^{-4}$	3.821905	6.141154
N7	$8.30 \cdot 10^{-4}$	$7.85 \cdot 10^{-5}$	0.451887	0.905952
N8	$1.28 \cdot 10^{-3}$	$1.16 \cdot 10^{-4}$	0.677334	1.349107
N10	$1.43 \cdot 10^{-3}$	$1.67 \cdot 10^{-4}$	0.562374	1.520077
G7	$1.36 \cdot 10^{-3}$	$1.65 \cdot 10^{-4}$	0.489736	1.441337
G6	$1.41 \cdot 10^{-3}$	$1.71 \cdot 10^{-4}$	0.520926	1.507413
Copper	$5.77 \cdot 10^{-6}$	$1.47 \cdot 10^{-6}$	0.004644	0.050341

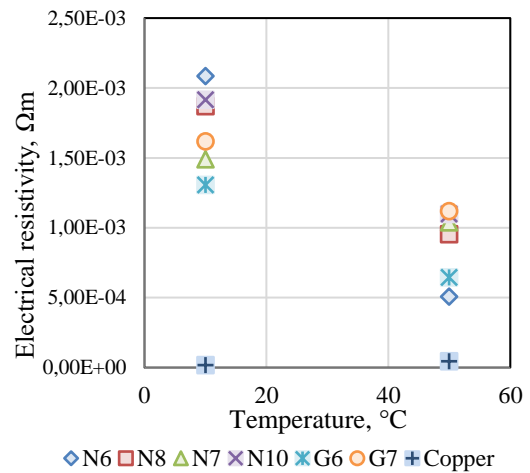


Fig. 6 Dependence of electrical resistivity of Ti-based samples on temperature

Table 5

Comparison of electrical resistivity obtained by different ways

Method	Highest electrical resistivity, Ωm	Lowest electrical resistivity, Ωm
Experimental	$2.27 \cdot 10^{-5}$	$6.4 \cdot 10^{-6}$
Found in similar research	$8.3 \cdot 10^{-6}$	$0.327 \cdot 10^{-6}$
Simulation of pure Ti sample	$3.46 \cdot 10^{-7}$	$3.46 \cdot 10^{-7}$

It was also observed that tested composite samples had an unusual behaviour, increase in resistivity while decreasing temperature. As seen in similar material research a

linear increase in resistivity is seen at a certain range. However, nonlinear behaviour can be exhibited at lower temperatures [15]. Measurements consisting of a wider range would be needed to determine if in fact this material behaves differently than other metals.

5. Conclusions

1. A design of the measurement setup was created using 3D modeling. The design conformed to needed requirements. Outer dimensions of the setup did not go over dimensions of the vacuum chamber. The outside dimensions of the measurement setup were 120 mm width, 228 mm length and 323 mm height. The samples fit into the sample holder and needles could probe them. The maximum sample diameter was 11 mm, and the minimum was 7 mm. The maximum sample thickness was 20 mm and minimum 4 mm. A heating and cooling element was applied. A minimum temperature of minus 55°C and a maximum temperature of 83°C could be achieved. The sample can be measured at different angles by rotating needle holder. Simulation was performed for the four-point probes with a pure titanium sample. Electrical resistivity calculated from simulation results showed a value of $3.46 \cdot 10^{-7} \Omega\text{m}$. The percentage error from true value was less than 10%.
2. Electrical resistance of titanium-based composite samples was measured. Electrical resistivity and conductivity were calculated. N6 sample had the highest resistivity with $2.27 \cdot 10^{-5} \Omega\text{m}$ and the N7 had the lowest with $6.40 \cdot 10^{-6} \Omega\text{m}$. Other samples had similar resistivity, around $1.2 \cdot 10^{-5} \Omega\text{m}$. Additionally, a copper sample was measured to verify the measurement. Result was $5.74 \cdot 10^{-8} \Omega\text{m}$, it was 3.3 times higher than the real value of copper. Additionally, all samples were tested at 10°C and 50°C. It was observed that all Ti-based composite samples had lower resistivity at 50°C, but copper sample had lower resistivity at 10°C. Experimental results were compared with similar results of other scientific research works. N7 sample and Ti_3AlC_2 had only 1.2 time difference. In all cases Ti-based composite samples had lower electrical conductivity than pure titanium.
3. The following experiments determining the investigation of electrical properties of Ti-based samples will be performed for the purpose to increase an accuracy of the testing of Ti-based samples with different chemical composition.
4. The project is in progress. Following future tasks as development, calibration, experimental research will allow to determine electrical properties of Ti-based composites with various chemical composition.

Acknowledgements

Presented work was performed with partial financial support from Research Council of Lithuania and Ministry of Education and Science of Ukraine in the framework of “Application of high-concentrated energy flows for producing nanostructured polyfunctional composite materials” joint project according to results of joint Ukrainian-Lithuanian R&D projects for the period of 2022 – 2023 contest (Reg. No. P-LUP-22-5).

Also, authors would like to express gratitude to the

Armed Forces of Ukraine for their bravery which made this work possible even in the dark times of war.

References

1. **Hayat, D.; Harshpreet, S.; Zhen, H.; Peng, C.** 2019. Titanium metal matrix composites: An overview. *Composites Part A. Applied Science and Manufacturing* 121: 418–438. <http://doi:10.1016/J.COMPOSITESA.2019.04.005>.
2. **Syzonenko, O.; Prokhorenko, S.; Lypyan, E. V.; Zaichenko, A. D.; Prystash, M. S.; Torpakov, A. S.; Pashchyn, M. O.; Voinarovska-Novak, R.; Sherehii, E.** 2020. Pulsed discharge preparation of a modifier of Ti–TiC System and its influence on the structure and properties of the metal, *Materials Science* 56(2). <http://doi:10.1007/s11003-020-00421-1>.
3. **Prihkna, T. A.; Ostash, O. P.; Kuprin, A. S.; Podhurska, V., Serbenyuk, T. B.; Gevorkyan, E. S.; Rucki, M.; Zurowski, W.; Kucharczyk, M. V.; Sverdun, V. B.; Karpets, M. V.; Ponomaryov, S. S.; Vasyliiv, B. D.; Moshchil, V. E.; Bortnitskaya, M. A.** 2021. A new MAX phases-based electroconductive coating for high-temperature oxidizing environment, *Composite Structures* 277(11): 46–49. <http://doi:10.1016/J.COMPSTRUCT.2021.114649>.
4. **Zhou, W.; Kang, L.; Jiaoqun, Z.; Ruguang, L.** 2018. In situ synthesis, mechanical and cyclic oxidation properties of $\text{Ti}_3\text{AlC}_2/\text{Al}_2\text{O}_3$ composites, *Advances in Applied Ceramics* 117(6): 340–346. <http://doi:10.1080/17436753.2018.1434953>.
5. **Moona, A.; Walia, R. S.; Rastogi, V.; Sharma, R.** Aluminium metal matrix composites: A retrospective investigation, *Journal of Chemical Technology and Metallurgy* 54(6): 1361–1370. Available from Internet: <https://core.ac.uk/download/pdf/229211628.pdf>.
6. **Zhou, D.; Qiu, F.; Wang, H.; Jiang, Q.** 2014. Manufacture of nano-sized particle-reinforced metal matrix composites: A review, *Acta Metallurgica Sinica (English Letters)* 27(5): 798–805. <http://doi:10.1007/s40195-014-0154-z>.
7. **Miccoli, I.; Edler, F.; Pfnur, H.; Tegenkamp, C.** 2015. The 100th anniversary of the four-point probe technique: The role of probe geometries in isotropic and anisotropic systems, *Journal of Physics Condensed Matter* 27(22). <http://doi:10.1088/0953-8984/27/22/223201>.
8. Test Probe GKS-100 291 090 A 2000 LP. Item GKS-100-1541. Available from Internet: <https://ingun.com/en-GB/GKS-100-291-090-A-2000-LP/GKS-100-1541>
9. **Fu, Z.; Mondal, K.; Koc, R.** 2016. Sintering, mechanical, electrical and oxidation properties of ceramic intermetallic TiC– Ti_3Al composites obtained from nano-TiC particles, *Ceramics International* 42(8): 9995–10005. <http://doi:10.1016/j.ceramint.2016.03.102>.
10. **Torres, C.; Quispe, R.; Calderon, N.; Eggert, L.; Hopfeld, M.; Rojas, C.; Camargo, M. K.; Bund, A.; Schaaf, P.; Grieseler, R.** 2021. Development of the phase composition and the properties of Ti_2AlC and Ti_3AlC_2 MAX-phase thin films – A multilayer approach towards high phase purity, *Applied Surface Science* 537: 147864. <http://doi:10.1016/J.APSUSC.2020.147864>.

11. **Peng, L. M.** 2077. Preparation and properties of ternary Ti_3AlC_2 and its composites from Ti-Al-C powder mixtures with ceramic particulates, *Journal of the American Ceramic Society* 90(4): 1312–1314. <http://doi:10.1111/j.1551-2916.2007.01517.x>.
12. **Gricius, D.** 2022. Design of experimental setup for measuring electrical conductivity of titanium composite samples, Master thesis. 60 p.
13. **Topsoe, H.** 1968. Geometric factors in four point resistivity measurement. 2nd revise. 64 p. Available from Internet: <https://www.iiserkol.ac.in/~ph324/StudyMaterials/GeometricFactors4ProbeResistivity.PDF>.
14. **Keithley.** 2016. *Low Level Measurements Handbook*. Book, vi, 1–5. Available from Internet: <http://goo.gl/dGoppA>
15. **Halim, J.; Persson, I.; Moon, E. J.; Kühne, Ph.; Darakchieva, V.; Persson, P. O. Å.; Eklund, P.; Rosen, J.; Barsoum, M. W.** 2019. Electronic and optical characterization of 2D Ti_2C and Nb_2C (MXene) thin films, *Journal of Physics Condensed Matter* 31(16). <http://doi:10.1088/1361-648X/ab00a2>.

D. Gricius, R. Kandrotaitė Janutienė, D. Mažeika, R. Šertvytis, O. N. Syzonenko, A. Torpakov

DEVELOPMENT OF DETERMINATION METHODOLOGY OF ELECTRICAL CONDUCTIVITY OF TITANIUM-BASED COMPOSITES

S u m m a r y

The Ti-based metal matrix composite samples are novel, fabricated by using high voltage electric discharge and spark plasma sintering processes. They have potential usage in the aviation industry. A research that allowed measuring an electrical conductivity of Ti-based composites was performed. A collinear four-point probe method was chosen for measurement of electrical conductivity. Needle-like probes were used to contact the tested sample. Other aspects of the measurement setup are discussed and selected according to relevant literature. A simulation was performed using COMSOL software to validate the measurement method. Furthermore, a simulation performed for contact force of the probes was performed. A 3D model of the measurement tool was created and designed. The measurement setup was tested and validated by using a copper sample. electrical resistance of Ti-based composite samples was measured, and electrical conductivity was calculated. Furthermore, samples were measured at different temperatures and resistivity dependence to temperature was presented. Experimental results are compared to similar research results.

Keywords: electrical conductivity, resistivity, four probe, MMC, composite.

Received September 7, 2022
Accepted April 5, 2023



This article is an Open Access article distributed under the terms and conditions of the Creative Commons Attribution 4.0 (CC BY 4.0) License (<http://creativecommons.org/licenses/by/4.0/>).